Molecular Human Reproduction pp. 1–8, 2007
Mol. Hum. Reprod. Advance Access published June 12, 2007 doi:10.1093/molehr/gam044

Dynamic expression of epoxyeicosatrienoic acid synthesizing and metabolizing enzymes in the primate corpus luteum

G. Irusta[1,3], M.J. Murphy[1], W.D. Perez[1] and J.D. Hennebold[1,2,4]

[1]Division of Reproductive Sciences, Oregon National Primate Research Center, Oregon Health and Science University, West Campus, Beaverton, OR 97006, USA; [2]Department of Obstetrics and Gynecology, Oregon Health and Science University, Portland, OR 97239, USA; [3]Present Address: Instituto de Biologia y Medicina Experimental (IBYME)-CONICET, Buenos Aires, Argentina.

[4]Correspondence address. Tel: +1 503 614 3720; Fax: +1 503 690 5563; henneboj@ohsu.edu

Epoxyeicosatrienoic acids (EpETrEs), produced from arachidonic acid via cytochrome P450 (CYP) epoxygenases, regulate inflammation, angiogenesis, cellular proliferation, ion transport and steroidogenesis. EpETrE actions are regulated through their metabolism to diols (dihydroxyeicosatrienoic acids; DiHETrE) via the enzyme soluble epoxide hydrolase (EPHX2). We set out to determine, therefore, whether EpETrE generating (epoxygenases *CYP2C8, 2C9, 2C19, 2J2, 1A2* and *3A4*) and metabolizing (EPHX2) enzymes are expressed in the primate corpus luteum (CL). CL were isolated from rhesus macaques during the early (day 3–5 post-LH surge), mid (day 6–8), mid-late (day 10–12), late (day 14–16) and very-late (day 17–19: menses) luteal phase of natural menstrual cycles. *EPHX2* mRNA levels peaked in mid-late CL (5-fold when compared with early CL, $P < 0.05$) and remained elevated in the late CL. Ablation of pituitary LH secretion and luteal steroid synthesis significantly reduced ($P < 0.05$) *EPHX2* mRNA levels in the mid-late CL, with progestin replacement being insufficient to restore its level of expression to control values. EPHX2 protein was localized to large and small luteal cells, as well as vascular endothelial cells. The EpETrE-generating CYP epoxygenase *2J2*, *2C9* and *3A4* genes were also expressed in the macaque CL. While *CYP2J2* mRNA levels did not significantly change through the luteal phase, *CYP2C9* and *CYP3A4* levels were significantly ($P < 0.05$) higher in the mid-late phase when compared with the early phase. CYP2C9, 2J2 and 3A4 proteins were each localized to the large luteal cells, with 2C9 and 2J2 also being present in the small luteal, stromal and endothelial cells. These studies demonstrate for the first time that an EpETrE generating and metabolizing system exists in the primate CL, with the latter being regulated by LH and steroid hormone(s).

Keywords: epoxygenase; epoxyeicosatrienoic acid; soluble epoxide hydrolase; ovary; corpus luteum

Introduction

It is well known that arachidonic acid can be converted to prostaglandins (PG) and leukotrienes via PG endoperoxide synthases (PGHS) and lipoxygenases, respectively. Additionally, certain cytochrome P450 (CYP) family members, collectively termed epoxygenases, convert arachidonic acid to four different regioisomers of epoxyeicosatrienoic acid (5,6-EpETrE; 8,9-EpETrE; 11,12-EpETrE and 14,15-EpETrE). The individual CYP epoxygenases, primarily belonging to the 2C and 2J family, preferentially form different EpETrE regio- and stereoisomers. EpETrEs, in turn, can be further metabolized to their corresponding vicinal diol (dihydroxyeicosatrienoic acids or DiHETrEs) via the enzyme soluble epoxide hydrolase (EPHX2).

EpETrEs affect numerous biological processes in a variety of different organ systems (Newman *et al*., 2005; Spector and Norris, 2006). For example, EpETrEs were reported to induce vasodilation and regulate vascular tone by activating large conductance K^+ channels (Hecker *et al*., 1994; Larsen *et al*., 2006). EpETrEs also limit endothelial inflammatory responses by inhibiting NF-κB activation, enhance fibrinolysis by increasing tissue plasminogen activator expression and regulate renal ion transport by controlling Na^+/K^+ transporter activity (Node *et al*., 1999,2001; Zhao and Imig, 2003). At the molecular and cellular level, EpETrEs were demonstrated to serve as critical intermediates in epidermal growth factor signaling, inhibitors of apoptosis and pro-mitogenic factors (Kroetz and Zeldin, 2002; Spector and Norris, 2006). In addition, depending on the cell type analysed, EpETrEs either elevated or inhibited PGHS-2 activity or expression (Peri *et al*., 1997,1998; Fang *et al*., 1998). The ability of the EpETrEs to affect the above-described processes is also dependent upon the level of EPHX2 activity as their conversion to DiHETrEs results in decreased biological potency (Fang *et al*., 1998; Spector and Norris, 2006).

Despite the wealth of information regarding EpETrE synthesis, metabolism and action in various tissues, little information exists regarding these activities in the ovary. Human granulosa cells obtained from IVF procedures were reported to produce and metabolize EpETrEs *in vitro* (Zosmer *et al*., 1990; Van Voorhis *et al*., 1993; Zosmer *et al*., 2002). Additionally, CYP epoxygenase expression, EpETrE production and EPHX2 expression were demonstrated in the porcine ovulatory follicle, where it was noted that the level of EpETrEs and their metabolites, particularly 11,12- and 14,15- isomers, corresponds with the level of follicular fluid estradiol (E_2) (Newman *et al*., 2004). Moreover, Van Voorhis and co-workers (1993) demonstrated that low doses (5–10 nM) of 14,15-EpETrE enhance E_2 levels, whereas higher doses (1–50 μM) reduce E_2 concentrations in human granulosa cell cultures.

We recently demonstrated that soluble *EPHX2* mRNA is expressed at high levels in the mouse preovulatory follicle and developing corpus luteum (CL) (Hennebold *et al*., 2005). A parallel increase in EPHX2 enzyme activity was noted throughout a stimulated estrous cycle with the highest levels of activity being observed in the post-ovulatory interval. We set out, therefore, to determine whether a similar EpETrE metabolizing system exists in CL obtained from rhesus monkeys, a species that possesses a long, well-defined luteal phase (Stouffer, 2004). Studies were also conducted to characterize the presence and regulation of the genes encoding EpETrE synthesizing enzymes in the macaque CL through the luteal phase of natural menstrual cycles.

Materials and Methods

Animals

The general care and housing of rhesus monkeys (*Macaca mulatta*) at the Oregon National Primate Research Center (ONPRC) was described previously (Wolf *et al*., 1990). All protocols were approved by the ONPRC Animal Care and Use Committee, and conducted in accordance with NIH Guidelines for the Care and Use of Laboratory Animals. Menstrual cycles of adult female rhesus monkeys were monitored daily. Six days after menses, daily blood samples were collected by saphenous venipuncture. Serum was collected, and stored at $-20^{\circ}C$, until assayed for E_2 and progesterone levels by specific electrochemiluminescent assays (Roche Elecsys 2010) through the Endocrine Services Laboratory, ONPRC (Young *et al*., 2002). The first day of low serum E_2 following the mid-cycle peak has been demonstrated to correspond with the day after the LH surge, and was therefore termed Day 1 of the luteal phase (Duffy *et al*., 1999).

Tissues

CL ($n = 3–4$ stage) were isolated from anesthetized monkeys during an aseptic ventral midline laparotomy as previously described (Duffy *et al*., 2000). CL were collected during the early (days 3–5 post-LH surge), mid (days 6–8), mid-late (days 10–12), late (days 14–16) and very-late (days 17–19; mense) luteal phase. Each CL was divided into thirds, with 2 out of the 3 portions being frozen in liquid N_2. The frozen samples were then stored at $-80^{\circ}C$ until they were used for RNA and protein isolation. The remaining portion of each CL was fixed in 10% neutral buffered formalin for 5–7 days (Richard-Allen Scientific, Kalamazoo, MI), dehydrated in a series of ethanol solutions (50, 70 and 100%) and stored after being embedded in paraffin.

Hormone ablation and replacement protocol

Hormone ablation and replacement was performed in adult rhesus monkeys beginning on day 9 of the luteal phase (mid-late) as previously reported (Young *et al*., 2004). In this treatment protocol, females were randomly assigned to one of five groups ($n = 4–5$/group): control (no treatment); antide (ANT) (GnRH antagonist, 3 mg/kg body weight, Ares Serono; LH ablation); ANT + recombinant human (rh)LH (40 IU tid; Ares Serono; LH replacement); ANT + rhLH + Trilostane (TRL; 600 mg, a 3β-hydroxysteroid dehydrogenase, or 3β-HSD, inhibitor from Sanofi Research; steroid ablation); ANT + rhLH + TRL + R5020 (2.5 mg, a nonmetabolizable progestin; Promegestone; DuPont/NEN; progesterone replacement). Serum E_2 and progesterone levels were analysed daily (Young and Stouffer, 2004). On day 12, CL were removed via laparotomy and flash frozen in liquid N_2. RNA was isolated using TRIzol (Invitrogen, Carlsbad, CA) according to the manufacturer's directions. RNA integrity was confirmed for each sample using an Agilent Technologies 2100 Bioanalyzer.

RT–PCR

Total RNA was isolated using TRIzol (Invitrogen) according to the manufacturer's directions. After RNA isolation, reverse transcription (RT) was performed on 1 μg DNase-treated RNA using Moloney murine leukemia virus reverse transcriptase (Invitrogen) for 1 h at 37°C. PCR was performed in a 25 μl volume using Clontech reagents and the following cycling parameters (MJ Research, Watertown, MA): initial denaturation, 94°C for 1 min; denaturation, 94°C for 30 s; annealing (see Table 1 for primer sequences and optimal annealing temperatures) for 45 s and primer extension at 72°C for 1 min. The number of cycles necessary to ensure a linear phase of amplification was determined empirically. PCR products (5 μl) were electrophoresed through a 1.7% agarose gel stained with 0.1 μg/ml ethidium bromide. Gels were visualized using a gel documentation system (Gel Doc 2000, BioRad, Hercules, CA) and subsequently analysed densitometrically with Quantity One software (BioRad). All values were normalized to the internal standard peptidylprolyl isomerase A (*PPIA*; also known as cyclophilin A).

Real-time PCR

PCR was performed using pooled luteal cDNA and primers designed against the human *EPHX2* gene (Table 1). The resulting rhesus macaque *EPHX2* PCR product was sequenced and used to design rhesus monkey-specific primers (Invitrogen) and a TaqMan© probe (Primer Express Software, Applied Biosystems, Foster City, CA) for the real-time PCR assay (for primer sequences see Table 1). The rhesus monkey *EPHX2* TaqMan© probe sequence was 5′-6FAM-ACTGGCCACCGCCCTCACTCTCT-TAMRA-3′. A matrix of varying primer concentrations was employed to determine optimal primer concentrations.

Real-time PCR was performed using the TaqMan© PCR Core Reagent Kit with the ABI PRISM 7700 Sequence Detection System (Applied Biosystems) as previously described (Young *et al*., 2002). 18S rRNA levels were monitored simultaneously in each sample to normalize the target signal. Amplifications were conducted in a 10 μl final volume containing 250 nmol/l TaqMan© *EPHX2* probe (labeled with the reporter dye FAM), 300 nmol/l *EPHX2* forward and reverse primers, 250 nmol/l TaqMan© 18S probe (labeled with the 5′ reporter dye VIC) and 50 nmol/l forward and reverse 18S primers. The PCR reactions were conducted in sealed 96-well optical plates with thermal cycler conditions of: 2 min at 50°C, 10 min at 95°C and 40 cycles of 15 s at 95°C (denaturation) and 1 min at 60°C (primer annealing/extension). An internal standard curve, generated from five 10-fold dilutions of cDNA pooled from all CL samples, was used for relative mRNA quantification. The RNA equivalent values were divided by complimentary 18S RNA equivalent values derived from the same internal standard curve.

Table 1: Oligonucleotide sequence and optimal annealing temperatures of PCR primers

Gene	Forward primer	Reverse primer	Annealing temperature (°C)
CYP3A4	5′ TGATGGCTCTAACAATGAC 3′	5′ TTCTAAACAATGGGCAAAG 3′	52
CYP1A2	5′ TCAAGCACAGCAAGAAGG 3′	5′ GGTTTACGAAGACACAGCA 3′	50
CYP2C19	5′ CTTGTGGAGGAGTTGAGA 3′	5′ CGAGGGTTGTTGATGTC 3′	50
CYP2C9	5′ CTTTATTGATTGCTTCCTGATG 3′	5′ GTAGCACAGAAGTCAGGGAAA 3′	60
CYP2C8	5′ GCAGGATAGGAGCCAC 3′	5′ TGTAGCACGGAAGTCAG 3′	51
CYP2J2	5′ TTTCTGCTCGCTGCTGACTTT 3′	5′ AACCTTCTTTGCTCCTTCCA 3′	60
EPHX2	5′ GAGTTGGTATTCTTGGAGG 3′	5′ TGTTGGGATTTGCTGG 3′	56
PPIA	5′ CCAGGGTTTATGTGTCAGGG 3′	5′ TGCCTTCTTTCACTTTGCCA 3′	56
EPHX2 real-time PCR	5′GGAGGTGTGCTGGTGTGGTA3′	5′ GGATTGCTGGTATGAAGGGAGTA 3′	60

Western blot

Proteins were extracted from individual CL samples by homogenization in lysis buffer (50 mM Tris–HCl, 150 mM NaCl, 10% glycerin and 1% Triton X-100) containing a protease inhibitor cocktail (Sigma, St. Louis, MO). Samples were centrifuged at 10 000*g* for 10 min at 4°C. The supernatant was collected and protein concentration was determined by Lowry assay (BioRad). Proteins (40 μg) were separated using 4–15% Tris–HCl sodium dodecyl sulfate-polyacrylamide gel electrophoresis and transferred onto nitrocellulose membranes. Rabbit polyclonal anti-human EPHX2 (kindly provided by Dr. Bruce Hammock, University of California, Davis, CA) and anti-human β-Actin (ACTB; Abcam, Cambridge, MA) were used at a 1:1000 dilution. ACTB antibody (1:5000 dilution) was used to verify equivalent protein loading. The blots were incubated for 1 h with peroxidase-conjugated anti-rabbit IgG antibody (1:4000; Santa Cruz Biologicals, Santa Cruz, CA) and the bands visualized using a chemiluminescent detection system (Santa Cruz Biologicals).

Immunohistochemistry

CL sections (6 μm) were deparaffinized with xylene and hydrated through a graded series of ethanol. Sections were incubated in phosphate-buffered saline (PBS) prior to pressure cooker antigen retrieval in citrate buffer (Citra; BioGenex Laboratories, Inc., San Ramon, CA). Endogenous peroxidase activity was then quenched with a 10 min incubation in 3% H_2O_2. Sections were placed in a blocking buffer (1.5% normal goat serum, NGS, in PBS) for 1 h at room temperature. Antibodies that recognize human CYP2C9 (Abcam, Cambridge, MA), CYP2J2 (kindly provided by Dr Zeldin DC, NIEHS), CYP3A4 (Abcam, Cambridge, MA) and EPXH2 were diluted to 1:100 in NGS/PBS and incubated with tissue sections at room temperature for 1 h or at 4°C overnight. Primary antibodies were detected using a biotinylated anti-rabbit IgG secondary antibody (7.5 μg/ml; Vector Laboratories) and a peroxidase substrate kit (ABC Elite Kit, Vector Laboratories). A non-specific, species and isotype-matched antibody was used as a negative control at the same concentration as the test antibody. The images were captured using an Olympus BX40 microscope equipped with a digital Olympus DP12 camera (40× and 100× magnification).

Statistical analysis

Statistical evaluation of mean differences among experimental groups was performed by ANOVA using the Sigma Stat software package (SPSS Inc., Chicago, IL). To isolate significant differences ($P < 0.05$) between groups, the Student–Newman–Keuls method was used for the pair-wise multiple comparisons.

Results

EPHX2 mRNA expression and protein immunolocalization in the rhesus macaque CL

We set out to determine whether *EPHX2* is highly expressed in the rhesus macaque CL as was observed in the developing mouse CL (Hennebold *et al*., 2005). Using primers generated from the human *EPHX2* gene sequence; *EPHX2* mRNA was also detected in the primate CL (data not shown). Moreover, real-time PCR analysis of *EPHX2* gene expression in the rhesus macaque CL revealed a significant increase in mRNA levels after the early luteal phase, with peak levels being observed in CL isolated from the mid-late luteal phase (5-fold relative to early CL, $P < 0.05$; Fig. 1A).

To determine whether there was a corresponding change in EPHX2 protein levels, western blot analysis was performed. In parallel with *EPHX2* gene expression, EPHX2 protein expression was minimal in homogenates isolated from early CL (Fig. 1B), but then increased to peak levels in mid-late and late CL.

The cellular distribution of EPHX2 was subsequently examined in the rhesus macaque CL by immunohistochemistry (IHC). Immunoreactivity was widely observed in the cells that comprise the CL, including the large luteal cells, and small luteal cells (Fig. 1C). Furthermore, EPHX2 expression was prominent in the endothelial cells lining individual blood vessels. The negative control (non-immune IgG) antibody exhibited no immunoreactivity (Fig. 1C, inset).

Regulation of EPHX2 gene expression in the rhesus macaque CL

Using a gonadotropin and steroid hormone ablation protocol, the regulation of *EPHX2* gene expression in the macaque CL at the mid-late stage (days 9–12 post-LH surge) of the luteal phase was investigated. CL isolated from LH depleted animals (e.g. ANT-treated), showed a significant reduction (2.9-fold, $P < 0.05$) in *EPHX2* gene expression when compared with untreated controls (Fig. 2). These levels were restored to control values after LH replacement, demonstrating a positive regulation of luteal *EPHX2* gene expression by LH. The administration of Trilostane (steroid depletion, a 3β-HSD inhibitor) to LH-replete animals (ANT + LH), however, inhibited *EPHX2* mRNA expression to levels observed in the ANT-only treatment group (Fig. 2). Reduced *EPHX2* gene expression in this group was not fully restored to control or ANT + LH levels following administration of a nonmetabolizable progestin (R5020). The analysis of circulating progesterone levels in the animals from which the individual CL were taken verified that the gonadotropin and steroid ablation and replacement treatments were effective for each group (data not shown, previously reported in Young and Stouffer, 2004).

Epoxygenase gene expression and protein localization in the rhesus macaque CL through the luteal phase

As the CYP epoxygenases are responsible for converting arachidonate to EpETrEs, an endogenous substrate for EPHX2, studies were conducted to determine if the epoxygenase genes are also expressed in the primate CL. PCR primers were generated that correspond to known primate epoxygenase genes (*CYP1A2, CYP3A4, CYP2C8, CYP2C9, CYP2C19* and *CYP2J2*) based on the available human sequences. Of these, one *CYP2J* (*CYP2J2*) and one *CYP2C* (*CYP2C9*) subfamily member was expressed in the primate CL (Table 2). A member of the *CYP3A* subfamily (*CYP3A4*) was also expressed in the rhesus macaque CL. Rhesus macaque liver was used as a positive control (Ikeya *et al*., 1989; Wrighton *et al*., 1993; Schuetz *et al*., 1994; Enayetallah *et al*., 2004), with all of the primer sets for each epoxygenase gene amplifying a product of the appropriate size. To ensure that each primer set successfully amplified the correct cDNA, each PCR product was sequenced and compared with the corresponding human epoxygenase gene. All rhesus macaque CYP epoxygenase gene products were 96–99% homologous to the corresponding human sequence (data not shown).

To determine if the *CYP2J2, 2C9* and *3A4* epoxygenase genes are differentially expressed in the rhesus macaque CL through the luteal phase, semi-quantitative RT–PCR was performed. Semi-quantitative RT–PCR was utilized in place of real-time PCR due to the fact that the high degree of homology shared between the *CYP* epoxygenase genes (95–99%) is problematic for designing specific real-time Taqman© probes and primers. Also, through the use of this methodology, amplification of the correct product was established by amplicon size as well as the subsequent sequencing of the PCR product. As such, *CYP2C9* expression was significantly higher ($P < 0.05$) during the mid-late luteal phase, when compared with the other stages of the luteal phase (Fig. 3). *CYP2J2* mRNA levels, however, did not differ between CL obtained from any of the different luteal stages analysed (Fig. 3). Epoxygenase *CYP3A4* expression in the rhesus monkey CL was significantly ($P < 0.05$) elevated in mid-luteal phase and remained high during mid-late and late stages when compared with early and very-late luteal phases (Fig. 3).

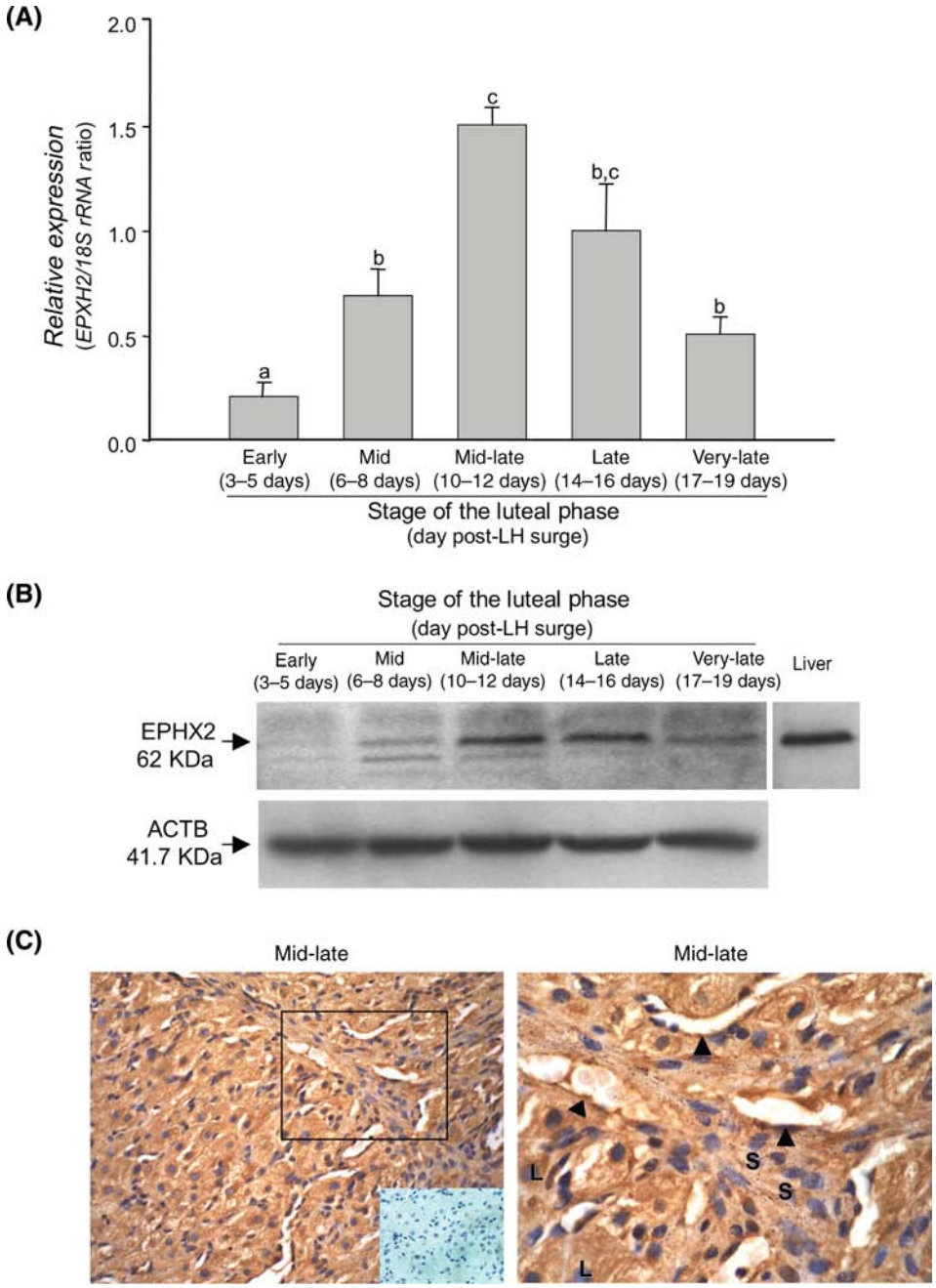

Figure 1: EPHX2 expression and immunolocalization in the rhesus macaque CL. **(A)** Quantitative real-time PCR analysis of *EPXH2* gene expression throughout the monkey luteal phase. As described in Materials and Methods, CL were collected during the early (days 3–5 post-LH surge), mid (days 6–8), mid-late (days 10–12), late (days 14–16) and very-late (days 17–19; menses) luteal phase. Data represent mean ± SEM and significant differences ($P < 0.05$) between the luteal phases are indicated by different letters. Values were standardized to internal 18S rRNA levels. **(B)** Western blot analysis of EPHX2 protein expression in homogenates generated from CL isolated at the different stages of the luteal phase. Liver was used as a positive control. **(C)** Immunolocalization of EPHX2 in rhesus macaque CL that were surgically removed during the mid-late luteal phase. L, large luteal cells; S, small luteal and stromal cells; arrowheads, endothelial cells lining blood vessels. Left panel: 40× magnification image. Right panel: 100× magnification of the boxed area indicated in the lower magnification (40×) image. A species and isotype-matched, non-immune antibody was used as a negative control at the same dilution as the test antibody (inset, mid-late CL).

To determine the potential cellular site of EpETrE synthesis within the primate CL, IHC was performed using antibodies that recognize human 2J2, 2C9 and 3A4 epoxygenases. IHC was performed using sections obtained from CL at the mid-late luteal phase, the stage at which a high level of expression for each epoxygenase gene was noted. Mid-late stage CL displayed positive CYP2C9 and 2J2 immunoreactivity within large luteal cells, small luteal and stromal cells, as well as endothelial cells lining blood vessels (Fig. 4A, B). CYP2C9 and 2J2 staining, while apparent in small luteal and stromal cells, was more intense in large luteal cells. CYP3A4 protein also localized predominantly in the large luteal cells, with limited expression present in the small luteal, stromal and endothelial cell populations (Fig. 4C).

Discussion

The *EPXH2* gene encodes soluble EPHX2, an enzyme, i.e. highly conserved between organisms (Newman *et al*., 2005) and is involved in the conversion of lipid epoxides (e.g. EpETrEs) to their corresponding

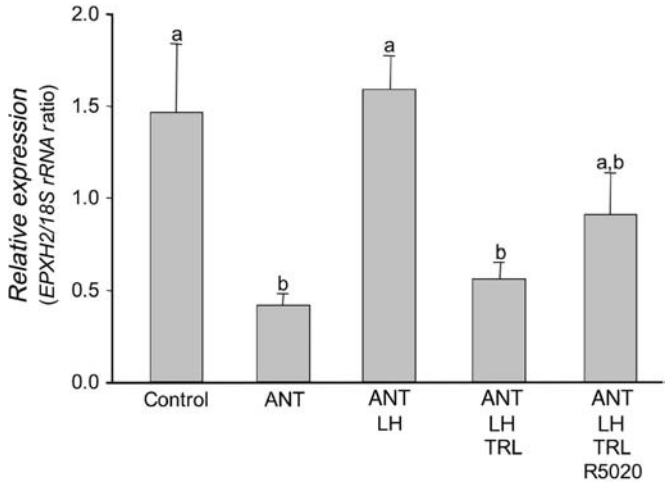

Figure 2: Regulation of *EPHX2* gene expression in the rhesus macaque CL Relative expression of the *EPHX2* gene was analysed by quantitative real-time PCR (mean ± SEM) throughout the luteal phase. CL were obtained from untreated (control) animals; or those undergoing gonadotropin and steroid ablation (ANT), gonadotropin replacement (ANT + LH), gonadotropin replacement with steroid ablation (ANT + LH + Trilostane or TRL) and gonadotropin plus progestin replacement (ANT + LH + TRL + R5020) protocols. Treatments were initiated during the mid-late luteal phase (day 9), with CL being isolated 3 days later (day 12). Values were standardized to the internal control 18S rRNA. Data represent mean ± SEM and significant differences ($P < 0.05$) between treatments and the untreated (control) animals are indicated by different letters.

vicinal diols (e.g. DiHETrEs) (Chacos *et al*., 1983; Beetham *et al*., 1995; Borhan *et al*., 1995; Yu *et al*., 2000). The EPHX2 enzyme serves to alter the EpETrE/DiHETrE ratio and, thus, the potential of these lipid epoxides to modulate various biological processes. In this regard, Fang *et al*. (1998) demonstrated that 14,15-EpETrE reduced PGE_2 formation in smooth muscle cells, whereas 14,15-DiHETrE was incapable of eliciting this effect. EpETrEs also serve as regulators of vascular tone through their capacity to hyperpolarize the underlying smooth muscle cells by activating large conductance K^+ channels (Hecker *et al*., 1994; Larsen *et al*., 2006). This vasodilatory effect has also been shown to be dependent on the level of endothelial cell EPHX2 activity and EpETrE metabolism (Imig *et al*., 2005).

Despite the increasing lines of evidence regarding the role of EpETrE formation and degradation in other tissues, little is known about the existence of an EpETrE synthesizing and metabolizing system in the ovary. Recently, we reported that the expression of the mouse *Ephx2* gene increased significantly just prior to and after ovulation in animals undergoing a stimulated estrous cycle (Hennebold *et al*., 2005). Studies were conducted, therefore, to extend these findings to primate CL isolated throughout the luteal lifespan

Table 2: Epoxygenase gene expression in rhesus macaque CL

Epoxygenase gene	Luteal expression	Liver expression[a]
CYP2C8	−	+
CYP2C9	+	+
CYP2C19	−	+
CYP2J2	+	+
CYP1A2	−	+
CYP3A4	+	+

[a]liver mRNA served as a positive control for epoxygenase gene expression, with the resultant PCR products being sequenced to verify their identity.

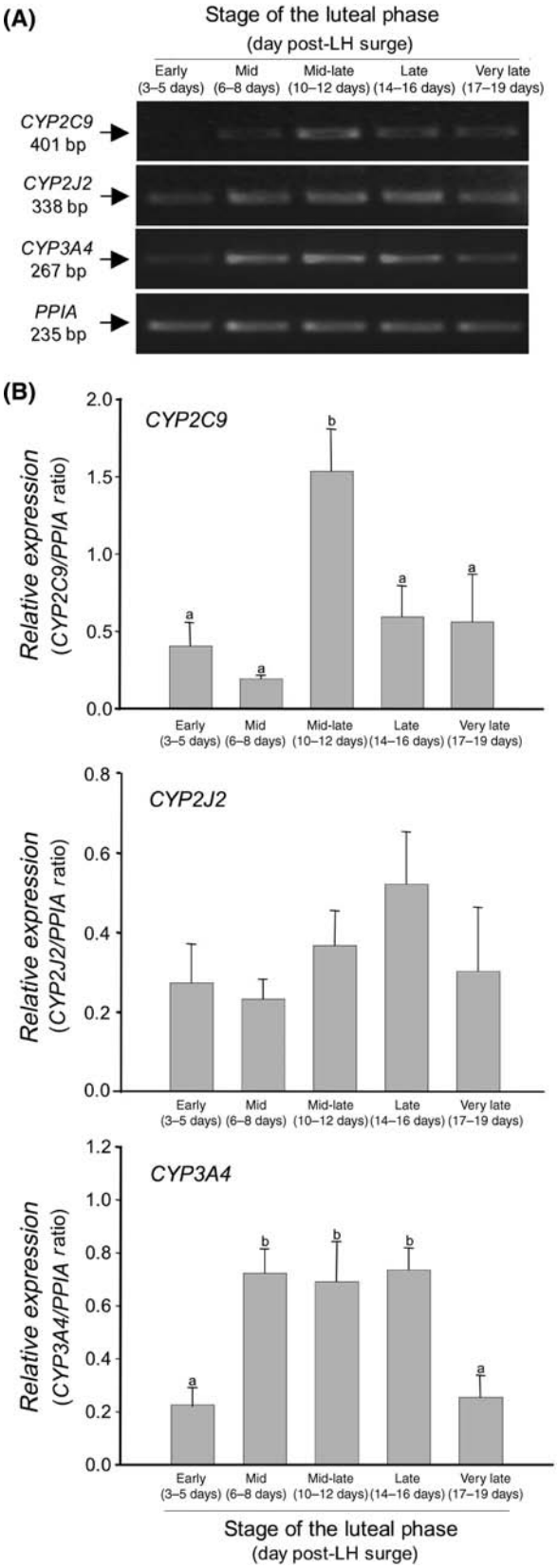

Figure 3: CYP epoxygenase mRNA expression in the rhesus macaque CL through the luteal phase. **(A)** A representative RT–PCR gel illustrating *CYP2C9* (401 bp), *CYP2J2* (338 bp) and *CYP3A4* (267 bp) gene expression in the rhesus macaque CL through the course of a natural luteal phase. *PPIA* (235 bp) amplification served as an internal control. **(B)** Densitometric values normalized to *PPIA*. Data are presented as the mean ± SEM ($n = 4–5$/stage). Different letters indicate significant differences ($P < 0.05$) between groups.

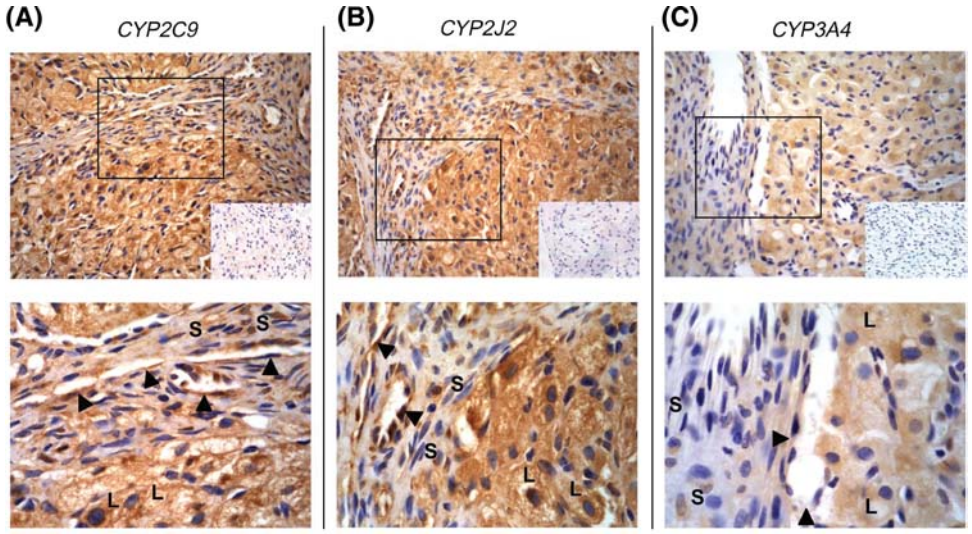

Figure 4: Immunolocalization of CYP epoxygenase proteins in the rhesus macaque CL. IHC for **(A)** CYP2C9, **(B)** CYP2J2 and **(C)** CYP3A4 was performed using sections obtained from rhesus macaque CL at the mid-late (days 10–12) stage of the luteal phase, a period of high gene expression for all three epoxygenases. L, large luteal cells; S, small luteal and stromal cells; arrowheads, endothelial cells lining blood vessels. Top panels: low power magnification (40×) images; Bottom panels: 100× magnification corresponding to the boxed area indicated in the top (low magnification) panels. Negative controls (insets) included using a species and isotype matched non-immune antibody in place of the specific anti-CYP antibody.

in the menstrual cycle. The expression of both *EPHX2* mRNA and protein peaked in the rhesus macaque CL during the mid-late and late luteal stages of the macaque menstrual cycle. The mid-late luteal phase is a point of transition between when the CL is at peak function (i.e. maximal progesterone synthesis) to the onset of its physiological regression (i.e. during the late luteal phase). Therefore, the induction of EPHX2 expression during the mid-late and late luteal phases suggests that this enzyme plays a role as an initiator and/or effector of luteal regression. In the mouse ovary, increased *Ephx2* gene expression after ovulation was observed primarily in luteinizing granulosa cells of the developing CL as determined by *in situ* hybridization (Hennebold *et al*., 2005). By immunohistochemical analysis, EPHX2 was localized to all cell types (e.g. large luteal, small luteal, stromal and endothelial cells) within the rhesus macaque CL.

Vertebrate *EPHX2* is an inducible gene product and a number of studies have demonstrated hormonal regulation (Denlinger and Vesell, 1989; Inoue *et al*., 1993; Inoue *et al*., 1995; Pinot *et al*., 1995). For example, hepatic EPHX2 enzyme activity in mice is under the control of the hypothalamic-pituitary-gonadal axis (Inoue *et al*., 1995). In the present study, we demonstrate for the first time that rhesus macaque *EPHX2* gene expression is regulated by the luteotropic hormone LH. Following the administration of the GnRH antagonist antide (ANT) to rhesus macaques for 3 days beginning on day 9 of the luteal phase, *EPHX2* mRNA expression was significantly inhibited. With the replacement of LH in ANT-treated animals, however, *EPHX2* mRNA levels were similar to those within CL taken from control animals. Moreover, ablation of steroid hormone synthesis through the administration of a 3β-HSD inhibitor (Trilostane) significantly reduced *EPHX2* gene expression to levels observed in CL obtained from gonadotropin-depleted (i.e. ANT-treated) rhesus monkeys. Supplemental progestin (R5020) only partially, but not significantly, restored *EPHX2* mRNA levels to control values. *EPHX2* gene expression, therefore, is likely indirectly regulated through steroid hormones other than progesterone, possibly including estrogens and androgens. A similar steroid dependent, but progesterone independent, regulation of gene expression in the rhesus monkey CL was reported for the metalloproteinase ADAMTS1 (a disintegrin and metalloproteinase with thrombospondin repeats-1; Young and Stouffer, 2004). Additional *in vivo* steroid ablation and replacement studies, along with *in vitro* luteal cell experiments, will be required to define which steroids are primarily involved in regulating luteal *EPHX2* gene expression. Furthermore, the partial restoration and variability of *EPHX2* gene expression taken from animals receiving R5020 may be due to the limited number of CL available for analysis ($n = 4$) and, as such, may require additional samples from animals undergoing steroid ablation and replacement protocols to resolve this issue.

Since the EpETrEs are the primary endogenous substrates for *EPHX2*, we subsequently determined whether the EpETrE generating enzymes are also expressed in the rhesus macaque CL. Primate epoxygenase encoding genes include *CYP2C8, 2C9, 2C19, 2J2, 1A2* and *3A4* (Rifkind *et al*., 1995; Wu *et al*., 1996; Zeldin *et al*., 1996; Bylund *et al*., 1998; Ayajiki *et al*., 2003). Previous studies demonstrated that ovarian samples taken from women of undetermined age and menstrual cycle stage express epoxygenase genes belonging to the CYP2C family (Klose *et al*., 1999). Additionally, cultured human granulosa cells possess an epoxygenase activity, that is up-regulated by LH (Zosmer *et al*., 1990). In the present study, the expression of the *CYP2J2, 2C9* and *3A4* genes were detected in the rhesus macaque CL using a semi-quantitative RT–PCR approach. It was noted that *CYP2C9* and *3A4* mRNA expression increases in the mid-late and mid-luteal phase, respectively, relative to CL isolated from the early luteal phase. In contrast to *CYP3A4* gene expression, *CYP2C9* drops at the late luteal phase. The *CYP2J2* gene is constitutively expressed throughout the luteal phase. Moreover, there was no significant change in epoxygenase gene expression in CL isolated from animals undergoing the gonadotropin and steroid hormone ablation and replacement protocol (data not shown). When the cellular localization of the CYP2J2, 2C9 and 3A4 proteins was determined by IHC at the mid-late stage of the rhesus macaque luteal phase (i.e. at a point of high levels of gene expression), it was noted that these three epoxygenases are mainly expressed in large luteal cells, with variable staining in small luteal cells and endothelial cells. More importantly, however, these results demonstrate an overlap in CYP2C9, 2J2 and 3A4 expression with EPHX2 expression in the large luteal cells of the rhesus macaque CL. Additionally, co-localization of EPHX2

with CYP2C9 and 2J2 in the endothelial cells of blood vessels indicates that EpETrE actions may play a role in luteal vascular function, with any activity being regulated by their metabolism to DiHETrEs. Overlapping cellular expression between EPHX2 and CYP2C9 was reported in a number of human tissues, including the uterus (Enayetallah *et al*., 2004), thereby providing a system by which the synthesis, metabolism and consequently EpETrE-dependent activities are tightly controlled at a cellular level.

To our knowledge, this is the first time that the enzymes responsible for EpETrE synthesis and metabolism have been characterized in the primate CL. As such, these studies suggest a role for EpETrE synthesis and metabolism in primate luteal physiology. The epoxygenase genes *CYP2C9* and *3A4* exhibit variable patterns of expression in the rhesus macaque CL, with *CYP2J2* being constitutively expressed throughout the luteal phase of natural menstrual cycles. EPHX2 expression, on the other hand, begins to increase in the mid-late luteal phase and plateaus when luteal regression starts to take place (i.e. late luteal phase). The changes in EpETrE synthesizing and metabolizing enzyme expression during the CL lifespan likely alter the EpETrE/DiHETrE balance and, thus, the degree to which luteal cell processes are regulated by the arachidonate-derived epoxides.

Processes regulated by EpETrEs in other tissues that may be critical for various aspects of luteal development, function and/or regression include angiogenesis, inflammation, endothelial cell function and apoptosis. Specifically, inhibition of apoptosis by EpETrEs occurs through the activation of the phosphatidylinositol 3-kinase Akt signaling pathway (Chen *et al*., 1999). The angiogenic effects of the EpETrEs were also shown to utilize this pathway (Pozzi *et al*., 2005; Wang *et al*., 2005; Zhang *et al*., 2006). EpETrEs serve as endothelium-derived hyperpolarizing factors that cause relaxation of the underlying smooth muscle cells of the vessels thereby increasing blood flow (Fisslthaler *et al*., 1999; Fisslthaler *et al*., 2000; Campbell *et al*., 2001; Pratt *et al*., 2001). Furthermore, in non-ovarian cells, EpETrEs regulate production of PG through the regulation of PGHS-2 expression or activity (Peri *et al*., 1997; Fang *et al*., 1998; Peri *et al*., 1998). Lastly, EpETrEs produced in the rhesus macaque CL may regulate steroidogenesis as each of the EpETrE isomers (5,6-, 8,9-, 11,12- and 14,15-EpETrE) have been shown to induce steroid synthesis in human granulosa cells and mouse Leydig MA-10 cells (Van Voorhis *et al*., 1993; Zosmer *et al*., 2002; Wang *et al*., 2006). The latter was attributed to an EpETrE-dependent induction of steroidogenic acute regulatory protein expression (Wang *et al*., 2006). The above-described EpETrE activities taken together with the data presented herein supports a role for these arachidonate-derived compounds in luteal physiology. As such, future studies are warranted to further define the processes that are affected by EpETrEs in primate luteal cells.

Acknowledgements

We are grateful for the contributions of the ONPRC Endocrine Services (Dr. Dave Hess), Imaging & Morphology (Barbra Mason) and Molecular & Cell Biology Core Laboratories (Yibing Jia). A special thanks to Dr. Richard Stouffer and coworkers for providing CL RNA from hormone ablation and replacement protocols. We also thank Dr. Stouffer for his comments and critique of the manuscript. The CYP2J2 and EPHX2 antibodies were kindly donated by Dr. D.C. Zeldin, NIEHS and by Dr B.D. Hammock, University of California-Davis, respectively. This work was supported by NICHD HD42 000, NICHD U54-18 185 and NCRR RR00 136. GI was supported through a Fogarty fellowship (NIH Fogarty International Center grant TW/HD-00 668 to P. Michael Conn).

References

Ayajiki K, Fujioka H, Toda N, Okada S, Minamiyama Y, Imaoka S, Funae Y, Watanabe S, Nakamura A, Okamura T. Mediation of arachidonic acid metabolite(s) produced by endothelial cytochrome P-450 3A4 in monkey arterial relaxation. *Hypertens Res* 2003;**26**:237–243.

Beetham JK, Grant D, Arand M, Garbarino J, Kiyosue T, Pinot F, Oesch F, Belknap WR, Shinozaki K, Hammock BD. Gene evolution of epoxide hydrolases and recommended nomenclature. *DNA Cell Biol* 1995;**14**:61–71.

Borhan B, Mebrahtu T, Nazarian S, Kurth MJ, Hammock BD. Improved radiolabeled substrates for soluble epoxide hydrolase. *Anal Biochem* 1995;**231**:188–200.

Bylund J, Ericsson J, Oliw EH. Analysis of cytochrome P450 metabolites of arachidonic and linoleic acids by liquid chromatography-mass spectrometry with ion trap MS. *Anal Biochem* 1998;**265**:55–68.

Campbell WB, Falck JR, Gauthier K. Role of epoxyeicosatrienoic acids as endothelium-derived hyperpolarizing factor in bovine coronary arteries. *Med Sci Monit* 2001;**7**:578–584.

Chacos N, Capdevila J, Falck JR, Manna S, Martin-Wixtrom C, Gill SS, Hammock BD, Estabrook RW. The reaction of arachidonic acid epoxides (epoxyeicosatrienoic acids) with a cytosolic epoxide hydrolase. *Arch Biochem Biophys* 1983;**223**:639–648.

Chen J-K, Wang D-W, Falck JR, Capdevila JH, Harris RC. Transfection of an active cytochrome P450 arachidonic acid epoxygenase indicates that 14,15-epoxyeicosatrienoic acid functions as an intracellular second messenger in response to epidermal growth factor. *J Biol Chem* 1999;**274**:4764–4769.

Denlinger CL, Vesell ES. Hormonal regulation of the developmental pattern of epoxide hydrolases. Studies in rat liver. *Biochem Pharmacol* 1989;**38**:603–610.

Duffy DM, Chaffin CL, Stouffer RL. Expression of estrogen receptor alpha and beta in the rhesus monkey corpus luteum during the menstrual cycle: regulation by luteinizing hormone and progesterone. *Endocrinology* 2000;**141**:1711–1717.

Duffy DM, Stewart DR, Stouffer RL. Titrating luteinizing hormone replacement to sustain the structure and function of the corpus luteum after gonadotropin-releasing hormone antagonist treatment in rhesus monkeys. *J Clin Endocrinol Metab* 1999;**84**:342–349.

Enayetallah AE, French RA, Thibodeau MS, Grant DF. Distribution of soluble epoxide hydrolase and of cytochrome P450 2C8, 2C9, and 2J2 in human tissues. *J Histochem Cytochem* 2004;**52**:447–454.

Fang X, Moore SA, Stoll LL, Rich G, Kaduce TL, Weintraub NL, Spector AA. 14,15-Epoxyeicosatrienoic acid inhibits prostaglandin E2 production in vascular smooth muscle cells. *Am J Physiol* 1998;**275**:H2113–H2121.

Fisslthaler B, Hinsch N, Chataigneau T, Popp R, Kiss L, Busse R, Fleming I. Nifedipine increases cytochrome P4502C expression and endothelium-derived hyperpolarizing factor-mediated responses in coronary arteries. *Hypertension* 2000;**36**:270–275.

Fisslthaler B, Popp R, Kiss L, Potente M, Harder DR, Fleming I, Busse R. Cytochrome P450 2C is an EDHF synthase in coronary arteries. *Nature* 1999;**401**:493–497.

Hecker M, Bara AT, Bauersachs J, Busse R. Characterization of endothelium-derived hyperpolarizing factor as a cytochrome P450-derived arachidonic acid metabolite in mammals. *J Physiol* 1994;**481**:407–414.

Hennebold JD, Mah K, Perez W, Vance JE, Stouffer RL, Morisseau C, Hammock BD, Adashi EY. Identification and characterization of an ovary-selective isoform of epoxide hydrolase. *Biol Reprod* 2005;**72**:968–975.

Ikeya K, Jaiswal AK, Owens RA, Jones JE, Nebert DW, Kimura S. Human CYP1A2: sequence, gene structure, comparison with the mouse and rat orthologous gene, and differences in liver 1A2 mRNA expression. *Mol Endocrinol* 1989;**3**:1399–1408.

Imig JD, Zhao X, Zaharis CZ, Olearczyk JJ, Pollock DM, Newman JW, Kim IH, Watanabe T, Hammock BD. An orally active epoxide hydrolase inhibitor lowers blood pressure and provides renal protection in salt-sensitive hypertension. *Hypertension* 2005;**46**:975–981.

Inoue N, Fujiwara K, Iwata T, Imai K, Aimoto T. Involvement of pituitary hormone in the sex-related regulation of hepatic epoxide hydrolase activity in mice. *Biol Pharm Bull* 1995;**18**:536–539.

Inoue N, Yamada K, Imai K, Aimoto T. Sex hormone-related control of hepatic epoxide hydrolase activities in mice. *Biol Pharm Bull* 1993;**16**:1004–1007.

Klose TS, Blaisdell JA, Goldstein JA. Gene structure of CYP2C8 and extrahepatic distribution of the human CYP2Cs. *J Biochem Mol Toxicol* 1999;**13**:289–295.

Kroetz DL, Zeldin DC. Cytochrome P450 pathways of arachidonic acid metabolism. *Curr Opin Lipidol* 2002;**13**:273–283.

Larsen BT, Gutterman DD, Hatoum OA. Emerging role of epoxyeicosatrienoic acids in coronary vascular function. *Eur J Clin Invest* 2006;**36**:293–300.

Newman JW, Morisseau C, Hammock BD. Epoxide hydrolases: their roles and interactions with lipid metabolism. *Prog Lipid Res* 2005;**44**:1–51.

Newman JW, Stok JE, Vidal JD, Corbin CJ, Huang Q, Hammock BD, Conley AJ. Cytochrome p450-dependent lipid metabolism in preovulatory follicles. *Endocrinology* 2004;**145**:5097–5105.

Node K, Huo Y, Ruan X, Yang B, Spiecker M, Ley K, Zeldin DC, Liao JK. Anti-inflammatory properties of cytochrome P450 epoxygenase-derived eicosanoids. *Science* 1999;**285**:1276–1279.

Node K, Ruan XL, Dai J, Yang SX, Graham L, Zeldin DC, Liao JK. Activation of Galpha s mediates induction of tissue-type plasminogen activator gene transcription by epoxyeicosatrienoic acids. *J Biol Chem* 2001;**276**:15983–15989.

Peri KG, Almazan G, Varma DR, Chemtob S. A role for protein kinase C alpha in stimulation of prostaglandin G/H synthase-2 transcription by 14,15-epoxyeicosatrienoic acid. *Biochem Biophys Res Commun* 1998;**244**:96–101.

Peri KG, Varma DR, Chemtob S. Stimulation of prostaglandin G/H synthase-2 expression by arachidonic acid monoxygenase product, 14,15-epoxyeicosatrienoic acid. *FEBS Lett* 1997;**416**:269–272.

Pinot F, Grant DF, Spearow JL, Parker AG, Hammock BD. Differential regulation of soluble epoxide hydrolase by clofibrate and sexual hormones in the liver and kidneys of mice. *Biochem Pharmacol* 1995;**50**:501–508.

Pozzi A, Macias-Perez I, Abair T, Wei S, Su Y, Zent R, Falck JR, Capdevila JH. Characterization of 5,6- and 8,9-epoxyeicosatrienoic acids (5,6- and 8,9-EET) as potent *in vivo* angiogenic lipids. *J Biol Chem* 2005;**280**:27138–27146.

Pratt PF, Li P, Hillard CJ, Kurian J, Campbell WB. Endothelium-independent, ouabain-sensitive relaxation of bovine coronary arteries by EETs. *Am J Physiol Heart Circ Physiol* 2001;**280**:H1113–H1121.

Rifkind AB, Lee C, Chang TK, Waxman DJ. Arachidonic acid metabolism by human cytochrome P450s 2C8, 2C9, 2E1, and 1A2: regioselective oxygenation and evidence for a role for CYP2C enzymes in arachidonic acid epoxygenation in human liver microsomes. *Arch Biochem Biophys* 1995;**320**:380–389.

Schuetz JD, Beach DL, Guzelian PS. Selective expression of cytochrome P450 CYP3A mRNAs in embryonic and adult human liver. *Pharmacogenetics* 1994;**4**:11–20.

Spector AA, Norris AW. Action of epoxyeicosatrienoic acids (EETs) on cellular function. *Am J Physiol Cell Physiol* 2006;

Stouffer RL. The functions and regulation of cell populations comprising the corpus luteum during the ovarian cycle. In: Leung PCK, Adashi EY (ed). *The Ovary*. : Elsevier Academic PressSan Diego, 2004,169–184.

Van Voorhis BJ, Dunn MS, Falck JR, Bhatt RK, VanRollins M, Snyder GD. Metabolism of arachidonic acid to epoxyeicosatrienoic acids by human granulosa cells may mediate steroidogenesis. *J Clin Endocrinol Metab* 1993;**76**:1555–1559.

Wang X, Shen CL, Dyson MT, Yin X, Schiffer RB, Grammas P, Stocco DM. The involvement of epoxygenase metabolites of arachidonic acid in cAMP-stimulated steroidogenesis and steroidogenic acute regulatory protein gene expression. *J Endocrinol* 2006;**190**:871–878.

Wang Y, Wei X, Xiao X, Hui R, Card JW, Carey MA, Wang DW, Zeldin DC. Arachidonic acid epoxygenase metabolites stimulate endothelial cell growth and angiogenesis via mitogen-activated protein kinase and phosphatidylinositol 3-kinase/Akt signaling pathways. *J Pharmacol Exp Ther* 2005;**314**:522–532.

Wolf DP, Thomson JA, Zelinski-Wooten MB, Stouffer RL. In vitro fertilization-embryo transfer in nonhuman primates: the technique and its applications. *Mol Reprod Dev* 1990;**27**:261–280.

Wrighton SA, Stevens JC, Becker GW, VandenBranden M. Isolation and characterization of human liver cytochrome P450 2C19: correlation between 2C19 and S-mephenytoin 4'-hydroxylation. *Arch Biochem Biophys* 1993;**306**:240–245.

Wu S, Moomaw CR, Tomer KB, Falck JR, Zeldin DC. Molecular cloning and expression of CYP2J2, a human cytochrome P450 arachidonic acid epoxygenase highly expressed in heart. *J Biol Chem* 1996;**271**:3460–3468.

Young KA, Hennebold JD, Stouffer RL. Dynamic expression of mRNAs and proteins for matrix metalloproteinases and their tissue inhibitors in the primate corpus luteum during the menstrual cycle. *Mol Hum Reprod* 2002;**8**:833–840.

Young KA, Stouffer RL. Gonadotropin and steroid regulation of matrix metalloproteinases and their endogenous tissue inhibitors in the developed corpus luteum of the rhesus monkey during the menstrual cycle. *Biol Reprod* 2004;**70**:244–252.

Young KA, Tumlinson B, Stouffer RL. ADAMTS-1/METH-1 and TIMP-3 expression in the primate corpus luteum: divergent patterns and stage-dependent regulation during the natural menstrual cycle. *Mol Hum Reprod* 2004;**10**:559–565.

Yu Z, Xu F, Huse LM, Morisseau C, Draper AJ, Newman JW, Parker C, Graham L, Engler MM, Hammock BD *et al.* Soluble epoxide hydrolase regulates hydrolysis of vasoactive epoxyeicosatrienoic acids. *Circ Res* 2000;**87**:992–998.

Zeldin DC, Moomaw CR, Jesse N, Tomer KB, Beetham J, Hammock BD, Wu S. Biochemical characterization of the human liver ' P450 arachidonic acid epoxygenase pathway. *Arch Biochem Biophys* 1996;**330**:87–96.

Zhang B, Cao H, Rao GN. Fibroblast growth factor-2 is a downstream mediator of phosphatidylinositol 3-kinase-Akt signaling in 14,15-epoxyeicosatrienoic acid-induced angiogenesis. *J Biol Chem* 2006;**281**:905–914.

Zhao X, Imig JD. Kidney CYP450 enzymes: biological actions beyond drug metabolism. *Curr Drug Metab* 2003;**4**:73–84.

Zosmer A, Elder MG, Sullivan MH. Production of intracellular arachidonic acid metabolites by human granulosa cells. *Prostaglandins Leukot Essent Fatty Acids* 1990;**41**:265–267.

Zosmer A, Elder MG, Sullivan MH. The production of progesterone and 5,6-epoxyeicosatrienoic acid by human granulosa cells. *J Steroid Biochem Mol Biol* 2002;**81**:369–376.

Submitted on April 16, 2007; resubmitted on May 8, 2007; accepted on May 14, 2007